



An effect of ionic liquids on polymorph transformations in polyvinylidene fluoride at its crystallization from solution

V. V. Kochervinskii¹ · N. V. Kozlova¹ · D. O. Ponkratov² · A. A. Korlyukov² · D. A. Kiselev³ · T. S. Ilina³ · Yu. S. Terekhova³ · N. A. Shmakova^{1,4} · A. I. Khorokhorin⁵

Received: 24 April 2019 / Revised: 24 July 2019 / Accepted: 25 July 2019 / Published online: 7 August 2019
© Springer-Verlag GmbH Germany, part of Springer Nature 2019

Abstract

According to IR spectroscopy data, crystallization of polyvinylidene fluoride from dimethylformamide and dimethylsulfoxide solutions at 100 °C and 80 °C is accompanied in the last case by the formation of polymorph modification mixtures of γ and β phases. In the presence of a number of ionic liquids, the same crystallization is accompanied by conformation transition in polymer chains from $T_3GT_3G^-$ to the conformation of a planar zigzag. We think that it takes place due to ion-dipole interactions between cations of the imidazole ring with fluorine atoms of polymer chains in the amorphous phase. X-ray data show that polar crystals of the β phase of non-doped polymer contain many conformational defects in the form of $T_3GT_3G^-$ isomers. At polymer doping with ionic liquid, the number of such defects is lowering. Due to this, the density of crystals formed grows. Conformation changes noted affect the signal of electromechanical response fixed by piezoresponse force microscopy. In particular, it has been shown that in the film under conditions of crystallization chosen process of self-polarization, which is registered by the method of Kelvin mode, takes place.

Keywords Ferroelectric polymers · Structure · Polarization · Piezoelectricity

Introduction

Polyvinylidene fluoride (PVDF) and its copolymers are related to the class of ferroelectric polymers which are widely used in various branches of technology [1–3]. It is known that polymorphism is typical of PVDF crystals, and there are at any rate 4 its modifications: α , β , γ , and α_p [1, 2, 4]. For ferroelectric

state formation, polar β phase has an important role since two chains of every elemental cell have the conformation of a planar zigzag. Earlier it was shown that the α phase, where two chains of a crystallographic cell with $TGTG^-$ conformation have dipole moments of opposite directions, is the most stable. Taking into account the important role of the polar β phase in the phenomena studied, $\alpha \rightarrow \beta$ transformation is usually realized by low-temperature uni-axial stretching of the film with α phase [1, 2, 4]. Another method of film crystallization is its polar modification by copolymerization of PVDF with tetrafluoroethylene or trifluoroethylene [1, 2, 5]. Introduction of oxide nanoparticles in PVDF also favors its crystallization in the polar β phase [6]. On the other hand, for modification of the chain structure of polymers, it is possible to use ionic liquids (IL) [7–9]. Recently, it was shown that ionic liquids may be utilized for modification of PVDF chain properties [9, 10]. In this work, with the use of the same polymer, an effect of ionic liquids of another type on processes of structure formation at PVDF crystallization from solution has been studied. It was shown that IL molecule structure may noticeably affect polymer polar modification formation. In particular, an increase in the flexible methylene link length

✉ V. V. Kochervinskii
kochval@mail.ru

¹ Karpov Institute Physical Chemistry, Vorontsovo pole 10, Moscow 105064, Russia
² A.N. Nesmeyanov Institute of Organoelement Compounds, Russian Academy of Sciences, Vavilova str. 28, Moscow 119991, Russia
³ National University of Science and Technology “MISIS”, Leninskiy pr. 4, Moscow 119049, Russia
⁴ Enikolopov Institute of Synthetic Polymeric Materials, Russian Academy of Sciences, Profsoyuznaya 70, Moscow 117393, Russia
⁵ Center of Unique Instrumentation RAS, Butlerova 15, Moscow 117342, Russia

(Merck, $\geq 95.0\%$) and 1-tetradecyl-3-methylimidazolium nitrate TdMImNO₃ (Merck, $\geq 95.0\%$) were dried at 55 °C/1 Torr, using a trap with P₂O₅, installed into a vacuum line; sodium nitrate (reagent grade) and DMF (Panreac, 99.8%) were used without additional purification. 0.12 g PVDF was dissolved in 3.6 ml DMF at 60 °C. If needed, 0.006 g of the filler (Im, sodium nitrate NaNO₃, BMImNO₃, or TdMImNO₃) was added. Films were prepared by isotherm crystallization at indicated temperatures from solutions on a glass plate by slow solvent evaporation. Thickness of films prepared was constant (12 μ m). IR spectra were recorded with a Bruker Equinox 55s spectrometer (with Fourier transform). Shooting was performed in transmission and attenuated total reflection ATR (diamond crystal) regimes; the latter was used to probe the 0.5–2- μ m-thick surface layer of polymer. Films formed had the same thickness. So, along with usual spectra, we could obtain difference spectra as well. The latter were obtained by subtraction spectra of doped films from those for films without additives.

Piezoresponse force microscopy (PFM), local polarization switching spectroscopy, and Kelvin probe force microscopy (KPFM) measurements were carried out with MFP-3D (Asylum Research, USA) and Ntegra Prima (NT-MDT, Russia) commercial scanning probe microscopes, using the CSG30/Pt conductive probe with the spring constant of 0.6 N/m. The drive amplitude for PFM scanning was 0.5 V, and frequency was 50 kHz (far from contact resonant). For KPFM measurements, the probe scanned the surface topography using a tapping mode. One-volt AC voltage was applied to the probe near its frequency (~ 48 kHz) to measure the sample surface potential distribution through a DC voltage feedback loop. All KPFM mappings were performed with the lift height of 30 nm, and 3-V DC voltage was applied to the probe. During the piezoelectric hysteresis loop measurements (remnant loops), an AC voltage was superimposed onto a triangular square-stepping wave ($f = 0.5$ Hz, writing time = read time = 25 ms, bias window were up to ± 170 V (for sample I) and ± 120 V (for sample V)). For the estimation of the piezoelectric constants (effective d_{33}), deflections and vibration sensitivity of the cantilever alignment were calibrated by GetReal procedure in IGOR Pro software (Asylum Research, USA).

Results

Such solvents DMF and DMCO, which have high affinity to PVDF, have been used in this work [11]. These solvents boil at high temperatures. That is why film crystallization can proceed only at high temperatures. In this connection, while using DMSO, it was checked whether crystallizing temperature may influence the microstructure of films formed. In Fig. 1, IR-spectra of films obtained at various temperatures are

presented. Analysis shows that crystallizing at 100 °C leads to the formation of predominantly non-polar crystals of the α phase, which have characteristic absorption bands [1, 2, 4]. It also follows from this figure that a decrease in film formation

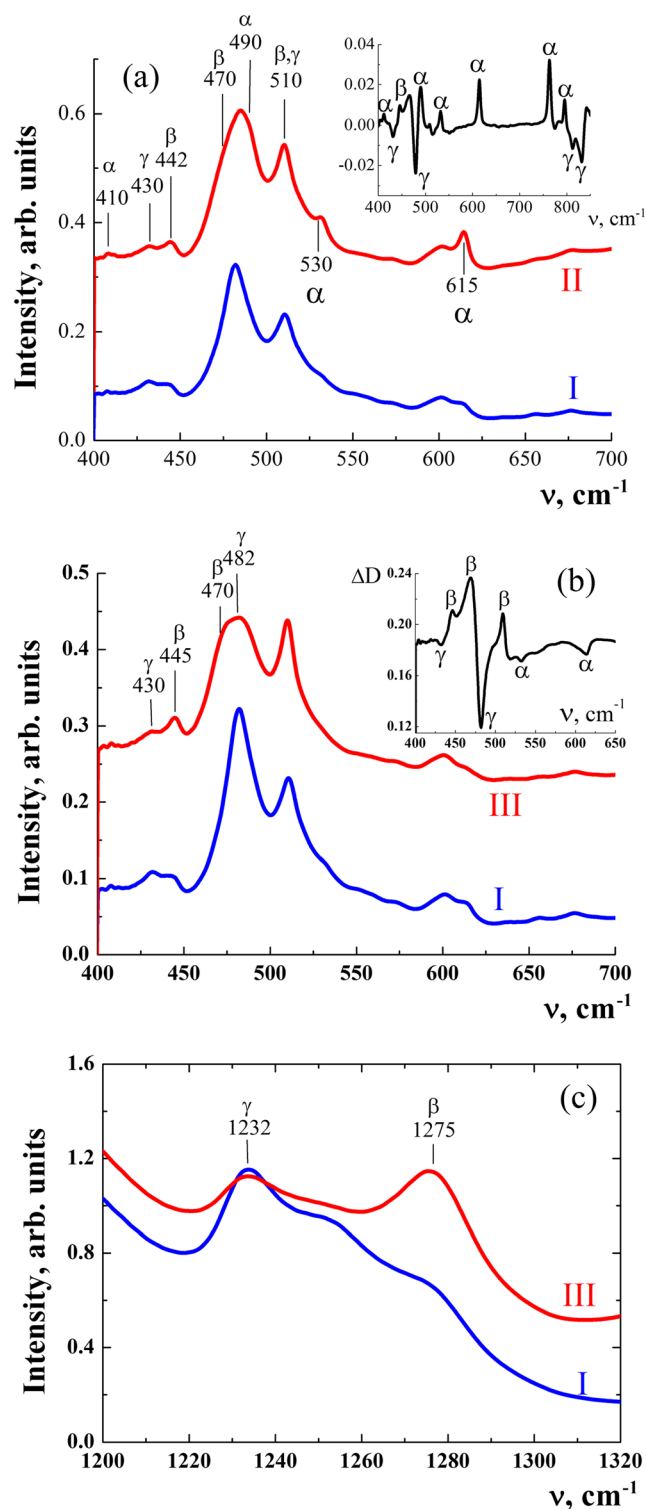


Fig. 3 IR spectra of PVDF films crystallized at 80 °C from their solutions in DMF (I), and with additives of imidazole II (a) and NaNO₃ III (b, c); insets in a and b are difference ATR spectra to sample I

temperature results in their crystallization as a mixture of β and γ phases [1, 2, 4]. The appearance of absorption bands marked in the figure characteristic of planar zigzag conformations (β phase) and $T_3GT_3G^-$ (γ phase) [1, 2, 4] indicates it. Qualitatively similar conclusion was made by authors of works [12–15].

IR spectroscopy gives information about the conformation of isomers which are present both in crystalline and amorphous phases. Since the proportion of the crystalline phase in polymers studied is not great ($\sim 50\%$), we wanted to assess the structure of crystals themselves. In Fig. 1d, X-ray diffraction patterns of the same films, which spectra are presented in Fig. 1, are shown. Analysis of the data obtained shows that crystallization at high temperatures results in the formation of non-polar crystals with chain conformation $TGTG^-$. Peaks from the film crystallized at low temperature indicate the formation of polar crystals of β and γ phases [1, 2, 4, 16, 17]. Non-trivial conclusion follows from these data: when ferroelectric polymer in polar modification crystallizes, chains in the amorphous phase have predominantly the same conformation as that in the crystal. Checking films formed at 80°C from PVDF solutions in DMF and DMSO showed that crystallization proceeds identically, i.e., with the formation of β and γ phases. From these data, it is possible to make the conclusion that, as applied to solvents chosen, crystallization temperature is a determining parameter for PVDF microstructure formation.

Investigation of an effect of ionic liquids IL introduced into PVDF solution has been carried out taking as an example the process of polymer crystallization from DMF solutions without IL under identical conditions (80°C). In Fig. 2, the structural formulae of dopants introduced are shown. It is seen that apart from imidazole and NaNO_3 , there are two ionic liquids IL which noticeably differ in the length of the flexible methylene link in position 1. As will be seen later, just the latter affects PVDF structure formation processes most of all. To determine the contribution of ionic centers in polymer crystallization process at films formation, apart from imidazole IL, non-charged Im was also tried. In Fig. 3a, the IR spectra of marked films are shown. It follows from them that Im introduction results in crystallization as the mixture of α and β phases. It is seen from difference absorption spectra, growing of bands responsible for PVDF chain conformation $TGTG^-$, a characteristic of non-polar α phase, is observed [1, 2, 4, 17–19].

As it follows from Fig. 3 b and c, the introduction of salt NaNO_3 into the crystallized film results in a change in the process of film crystallization. From the difference spectrum of the film formed (see inset in Fig. 3b), it can be clearly observed. As compared with spectra of films synthesized without NaNO_3 addition, in case of salt introduction, intensities of bands related to the γ phase (430 and 482 cm^{-1}) and α phase (530 and 615 cm^{-1}) of films formed decreased while those related to bands sensitive to the conformation of the

planar zigzag (442 , 510 , and 470 cm^{-1}) increased. A change in the ratio of intensities of bands 1232 and 1275 cm^{-1} (Fig. 3c) leads to the same conclusion.

According to literature data [1, 2, 4, 18, 19], bands 430 , 482 , and 1232 cm^{-1} should be attributed to chain conformation $T_3GT_3G^-$ in the γ phase crystals. Thus, the

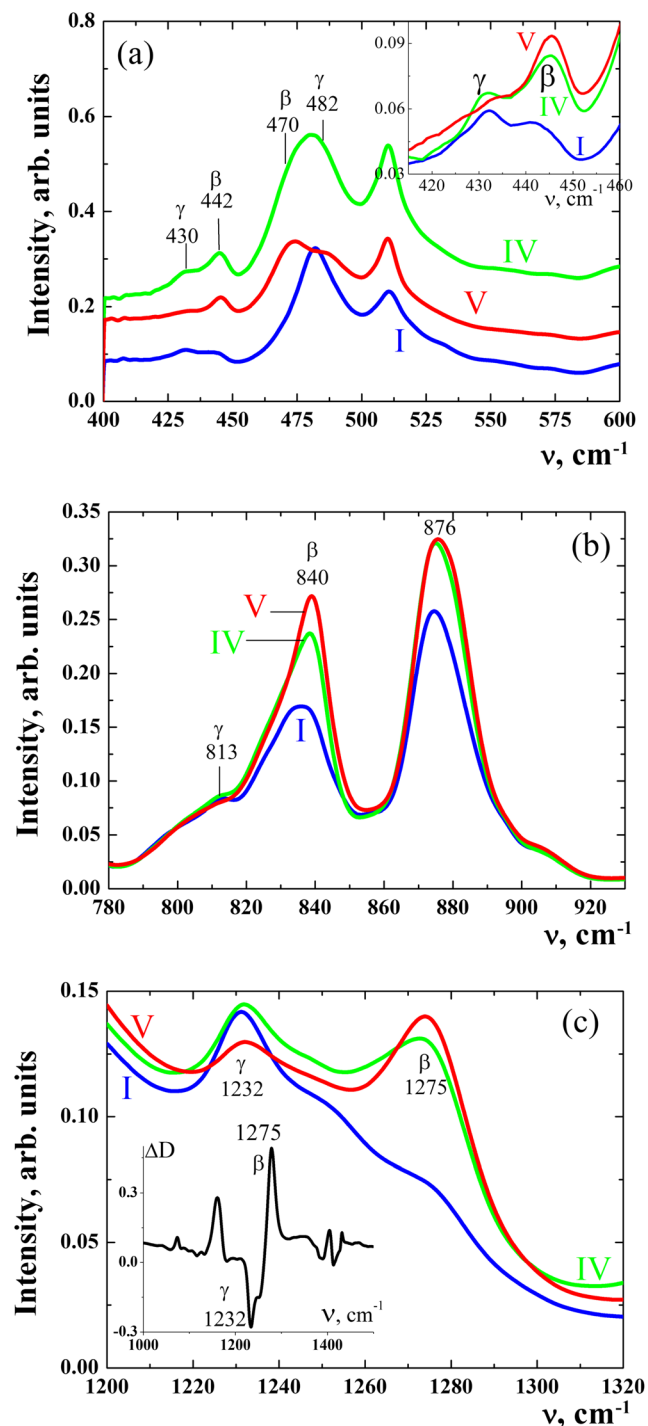


Fig. 4 IR spectra of PVDF films crystallized at 80°C from solutions in DMF (I) and with additives BMImNO_3^- (IV) and TdMImNO_3 (V) in the spectral diapason $400\text{--}600$ (a), $780\text{--}930$ (b), and $1200\text{--}1320$ (c) cm^{-1} ; ATR spectra are presented in the inset in a

introduction of the salt noted leads to shifting of conformational equilibrium between isomers $T_3GT_3G^-$ and a planar zigzag to the side of increasing of the latter. According to our opinion, such a different influence of two additives on PVDF structure formation may be due to the fact that salt introduced in the initial solution is in the form of ions concentration of which is determined by its dissociation degree. These ions are sources of the local electric field in a crystallized solution of extremely polar polymer. That is why they may affect the structure formation of the terminal structure. Data on an effect of outer electrical fields on phase transformations in considered polymers where polymorphism effects are strongly expressed [20]. Taking into account these data, let us consider an effect of BMImNO₃ and TdMImNO₃ additives on PVDF crystallization processes noted above. Their detailed elaboration can be seen in Fig. 4. It follows from the figure that with respect to the initial film, considerable differences in their IR spectra are observed. The same takes place in the case of NaNO₃ additive. From the comparison of these data with those for the film doped by Im (Fig. 3a), it follows that molecule transition from the neutral condition into cationic one (Fig. 2) must be responsible for this fact. It is also interesting to follow the role of IL chemical structure in the process of the film structure formation. Figure 4 data show that for all conformation sensitive bands, the same regularity is observed. PVDF film crystallization in the presence of IL TdMImNO₃ (V) is accompanied by a more considerable conformational transformation $T_3GT_3G^- \rightarrow (-TT)_n$. It is reflected quantitatively by the data on ratios of optical absorption bands mentioned above (Table 1). In Table 2, characteristics of difference spectra for conformation sensitive absorption bands for all kinds of dopants are presented. Let us remember that difference spectra for films of the same thickness were registered when the spectrum of the non-doped film obtained from DMF solution was used as a “standard.” It can be seen that for all pairs of bands differences calculated grow regularly in dopants series II \rightarrow III \rightarrow IV \rightarrow V. It follows from Table 2 that bands chosen characterize conformations of a planar zigzag (decreased) and $T_3GT_3G^-$ (subtracted). That is why this difference characterizes completeness of conformational transition

$T_3GT_3G^- \rightarrow (-TT)_n$ at this or that dopant. It follows from Table 2 that transition noted is the weakest for imidazole 2, and its maximum is in the case of cationic ionic liquids. It also follows from the table that an increase in the length of the flexible methylene link in position 1 of the imidazole ring increases conformational transition to its maximum. This is a new result which was not noted previously.

Discussion

Consideration of data obtained should be done not only for systems formed by crystallization from a solution like in our case. Indeed, there is a group of works where structural properties of composites on the base of PVDF are discussed. For example, it has been found that at the introduction of organically modified nanoparticles of clay [21–27] or ferrite nanoparticles [28–30], crystallization proceeded in polar β modification. It should be remembered that at usual crystallization from melt, homopolymer is formed in the non-polar phase. Analysis of data on z-potential of ferrite nanoparticles showed that they carry a negative charge [29]. In case of crystallization from solutions [9, 10, 31, 32], ionic liquid IL introduced will dissociate and in this way will generate carriers of charges. Therefore, all conclusions from cited works should be interpreted from the common position of ion-dipole interactions since PVDF contains in its chains CF₂ groups with great dipole moments. According to conclusions of authors of works [28–30], the negative charge on the surface of ferrite nanoparticle interacts with dipole moments of CH₂ groups of PVDF chains. Due to this, the latter crystallizes to the polar β phase. As for crystallization from solvents, our data do not confirm this hypothesis. IL studied by us contains imidazole cation and NaNO₃⁻ anion. If anions were determining in their influence on PVDF crystallization, the extent of $\gamma \rightarrow \beta$ transformation would be maximal in the case of polymer doping by NaNO₃ salt in a solvent. Indeed, at the same weight proportion of the dopant and the same dissociation extent, anion concentration in this case will be maximal and accordingly, $\gamma \rightarrow \beta$ transformation must be more pronounced. Table 1 data do not confirm this. More to it, transformation noted turns out to be maximal in case of dopant V, for which NO₃⁻ concentration will be minimal (Fig. 2). To our opinion, the predominant role in

Table 1 Intensity ratios of conformation sensitive absorption bands in PVDF films at their crystallizing from DMFA (I) solution and in the presence of various dopants

Dopant	Designation	D_{442}/D_{430}^*	D_{470}/D_{482}^*	D_{840}/D_{876}	D_{1275}/D_{1232}^*	D_{510}/D_{600}
–	I	0.90	0.40	0.41	0.60	6.0
Imidazole	II	1.20	0.58	0.63	1.20	
NaNO ₃	III	1.70	0.72	0.54	1.80	
BMImNO ₃	IV	1.85	0.77	0.76	1.60	
TdMImNO ₃	V	2.50	1.30	0.81	2.02	9.3

* Bands in numerator and denominator relate to the conformation of a plane zigzag and $T_3GT_3G^-$, respectively

Table 2 Structure formation parameters according to the data of differential spectra for PVDF films crystallized at 80 °C from DMF solutions with various dopants

Dopant	$\Delta (D_{442} - D_{430})$	$\Delta (D_{470} - D_{482})$	$\Delta (D_{842} - D_{813})$	$\Delta (D_{1275} - D_{1232})$
II	0.016	0.038	0.021	0.031
III	0.027	0.117	0.186	0.521
IV	0.041	0.130	0.302	0.650
V	0.046	0.16	0.346	0.770

crystallization process belongs to imidazole cation. Its ion-dipole interaction with fluorine atoms in PVDF chains will be determined because the value of the CF_2 group dipole moment (2,1 D) is more than an order of magnitude higher than that for the CH_2 group.

It is possible to find the definite proof of interactions noted by comparison of our data with those of authors of work [33]. IR spectra of cationic IL like in our case, but with anion PF_6^- have been studied there. In this connection, it is interesting to correlate the frequency positions of our IL characteristic bands and those from work [33]. These data are presented in Table 3 from which it follows that in the case of anion PF_6^- , frequencies of bands responsible for vibrations in inorganic cation are shifted to higher frequencies as compared with those of IL. Somewhat earlier, the same result was also obtained by authors of work [34]. More to it, it was shown that values of high frequency shift depend on the number of F atoms in the anion. Thus, it follows from considered data that fluorine may considerably influence vibration states of imidazole cation fragments [33, 34]. In our case, where fluorine is also present in polymer chains, it is interesting to compare absorption bands observed in IL IV before and after introduction it in PVDF. These data are also presented in Table 3. At comparison of frequencies in the first and last but one column, it is seen that after the introduction of IL in PVDF, bands turn out to be shifted to higher frequencies. This shift is about the same as if in our IL anion (NO_3^-) is replaced by PF_6^- (Table 3). Thus,

the presence of F atoms which are strong electron acceptors in the PVDF chain affects vibration level energy of ionic liquid IL introduced.

Accordingly, the data presented indicate that when PVDF crystallizes in the presence of cationic ionic liquids, interactions of cations with fluorine atoms are determining. Just because of such interactions, polymer chains obtain planar zig-zag conformation during crystallization. There is a separate question, why an increase in methylene link length in IL results in more complete transition $\gamma \rightarrow \beta$. To our opinion, it may be explained qualitatively taking into account stereochemical effects. As it follows from Fig. 2, imidazole cation in IL IV has two methyl groups which are known to have strong stereo-chemical hindrances at packing in a condensed state. Because of this, ion-dipole interactions cannot take up a compact position near fluorine atoms in the chains of PVDF amorphous phase. If methylene link length increases in ring position 1 at the transition from BMImNO_3 to TdMImNO_3 , stereo-chemical hindrances will partially decrease. It proceeds because the potential barrier for a methylene group rotation around C–C axis of the side chain is low. Due to this, imidazole cation has higher probability to be closer to fluorine atoms, and higher ion-dipole interactions will strengthen conformation transition $\gamma \rightarrow \beta$, that is observed experimentally. Apparently, this effect will compensate for partial decreasing of imidazole ring cation concentration at the transition from dopant IV to V, since their weight proportion was the same.

Table 3 Frequencies and shifts of main absorption bands in ionic liquid 1-butyl-3-methylimidazolium nitrate BMImNO_3^- (IV) and 1-butyl-3-methylimidazolium hexafluorophosphate $\text{BMImNO}_3\text{PF}_6^-$ [33], as well as those at introduction of (IV) in PVDF

BMImNO_3^- IV ν , cm^{-1}	BMImPF_6^- [33] ν , cm^{-1}	BMImPF_6^- – BMImNO_3^- $\Delta\nu$, cm^{-1}	Attribution	IV + PVDF ν , cm^{-1}	IV + PVDF –IV $\Delta\nu$, cm^{-1}
1165	1170	+5	$\nu (\text{CH}_3\text{--N})$	1167	+2
1457	1467	+10	$\nu (\text{CH}_3\text{--N})$ δCH_2 δCH_3	1469	+12
1560			ν	1568	+8
1565	1568	+3	Imidazole	1575	+10
1571	1576	+5	Ring	1585	+14
2872	2879	+7	νCH_2	2880	+8
2933	2939	+6	νCH_3	2940	+7
2958	2968	+10		2966	+8
3091	3122	+31	Fermi resonance	3120	+29
3143	3170	+27	$\nu \text{CH} + \text{ring}$	3170	+27

As noted, the introduction of imidazole (II) into the crystallized system gives a minimal effect for the considered conformational transition. But from Fig. 3a and Table 1, it follows that imidazole, however, also increases the proportion of chains in the conformation of the planar zigzag. This may be due to the formation of hydrogen bonds between protons in imidazole (Fig. 2) and fluorine atoms in CF_2 groups according to the type of $\text{NH} \dots \text{FC}$. This kind of interaction may also stabilize the conformation of the planar zigzag. The correctness of this hypothesis was previously proved when the doping of copolymers VDF with rhodamine 6G dye was studied [35, 36].

As it has been noted in the introduction, the polymer studied is a ferroelectric, and piezoelectricity realized in it is used in sensors of various kind [1–3]. In this connection, it is interesting to follow how this structure modification may affect its piezoelectrical characteristics. For this aim, the method of local piezoresponse force microscopy was chosen. Since polar crystals are included in the domain which can be registered by this method, it is interesting first to check how the above conformational transition will affect such crystals characteristics. It is seen in Fig. 5, from which it follows that PVDF crystallizing in the presence of dopant IV results in shifting of main reflex 110,200 of γ and β phases to higher angles. It means that the packing density of crystals formed in the presence of IL turns out to be higher. The following structure formation scheme seems the most probable. In a non-doped film, crystals of the β phase contain many defects in the form of $\text{T}_3\text{GT}_3\text{G}^-$ isomers that is known from IR spectroscopy data. Doping leads to falling down a number of such defects in crystals. It will be understood as conformational transition $\text{T}_3\text{GT}_3\text{G}^- \rightarrow (-\text{TT})_n$, which we register by the method of IR spectroscopy. Since the packing density of crystals of γ phase with conformation $\text{T}_3\text{GT}_3\text{G}^-$ is lower than that for crystals of β phase with the conformation of a planar zigzag [4, 16, 17],

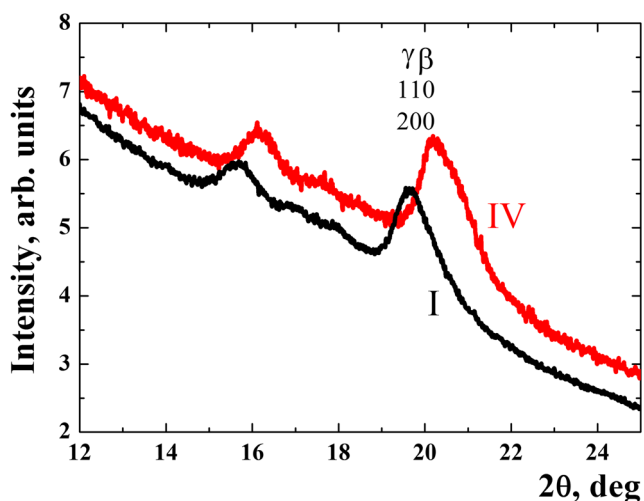


Fig. 5 X-ray diffraction curves of PVDV film samples crystallized from DMF solutions without dopant I and with ionic liquid (IV)

peaks observed must shift to greater angles. Just this is observed in the experiment (see Fig. 5).

Topography images of the tested area ($8 \times 8 \mu\text{m}^2$) of polymer films are presented in Fig. 6 a and b. The computed root mean square (RMS) roughness of the investigated area, and it is 4.4 nm for the initial sample (sample I) and 5.2 nm for polymer doped with IL (sample V). Figure 6 presents typical vertical (c and d) and lateral (e and f) piezoresponse signals as well as piezoresponse signals at second harmonic (g and h) for sample I (Fig. 6c, e, and g) and sample V (Fig. 6d, f, and h). Vertical PFM contrast is roughly proportional to the effective d_{33} coefficient and is determined by the projection of the polarization vector P on the normal to the polymer surface. On the other hand, the lateral piezoresponse image reflects the effective shear d_{15} , d_{24} piezoelectric coefficient proportional to the corresponding in-plane component of the polarization. For second harmonic, the cantilever oscillation in a contact mode scanning probe microscopy is used to determine local electrostrictive properties [37, 38].

Histograms of the vertical, lateral, and second harmonic PFM images are shown in Fig. 7 a and b for pure and doped polymer films, respectively. The peak distribution maximum corresponds to the most probable domain configurations, and its width reflects the number of available domain states. It can be noticed that these histograms possess symmetric shapes (gauss distribution) with peak maxima appearing at either positive (only for the vertical PFM image for the pure polymer film, sample I) or negative side with respect to the zero piezoelectric response value. Moreover, the appearance of non-zero piezoresponse in these samples in the unpoled state implies the existence of self-polarization in the samples. Analysis of histograms shows that effective local vertical (d_{33}) and lateral (d_{15} , d_{24} [39, 40]) piezoelectric coefficients and the second harmonic signal is the largest for the pristine polymer (sample I) film (Fig. 7).

As it is known, the latter is responsible for electrostriction phenomenon which for polymers studied makes a considerable contribution to macroscopic piezo-response [39–42]. As it follows from works [39, 40], the amorphous phase of considered polymers is responsible for electrostriction. It is understood from the general expression for piezoconstant d :

$$d = \frac{\partial D}{\partial X} = \frac{\partial \epsilon'}{\partial X} \epsilon_0 E + \epsilon' \epsilon_0 \frac{\partial E}{\partial X} + \frac{\partial P}{\partial X} \quad (1)$$

where D and X are electrical displacement and external mechanical stress and E , ϵ' and P are field, dielectric permittivity, and spontaneous polarization, respectively. The first term is responsible for electrostriction. The high value of the derivative $\frac{\partial \epsilon'}{\partial X}$ may be realized only at the expense of orientation polarization of amorphous phase chains when the polymer is at the temperature higher than its glass point. The higher the

proportion of the amorphous phase, the higher the electrostriction contribution is expected to be. Comparison of curves on the second harmonic (Fig. 7) shows that the signal intensity in the film with IL (V) turns to be about 3 times lower than that in the non-doped film (I). This may be qualitatively explained by the fact that in the amorphous phase chains in conformation $T_3GT_3G^-$ are less equilibrated with regard to external influence than those with the conformation of a planar zigzag [1, 2, 4, 43]. If aforesaid is true, in the sample crystallized in the presence of IL, crystallinity is expected to be higher. With the use of IR spectroscopy, we checked this supposition.

In Table 1, ratios of optical densities of “crystallinity” bands (840 and 510 cm^{-1}) and those of “amorphity” (600 и 876 cm^{-1}) [1, 2, 4] are presented. Indeed, it is seen that for both pairs of bands PVDF crystallization in the presence of IL V is accompanied by an increase in crystallinity. From Fig. 7, it also follows that electrostriction contribution has negative values in both films. It agrees qualitatively with data of other authors [41]. In this connection, the electrostriction contribution in piezoresponse will depend on the concentration of T_3GT_3G isomers. Since their proportion is lowering at PVDF crystallization in the presence of ionic liquid (Tables 1 and 2), the value

Fig. 6 Surface topography (a, b) and signals of vertical (c, d) and lateral (e, f) piezoresponse on the main frequency as well as on the second harmonic (g, h) in the initial sample (I) and after ionic liquid introduction (V)

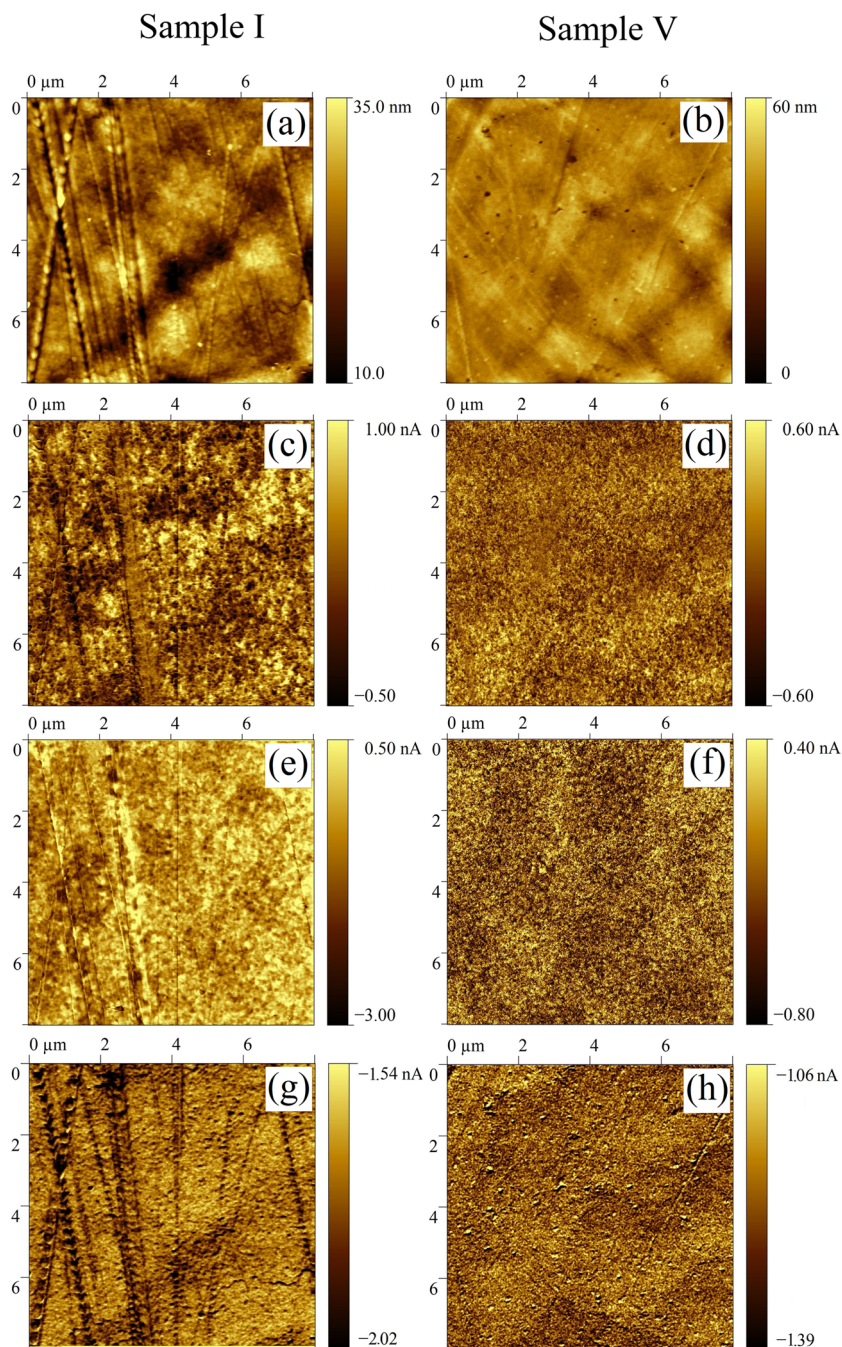
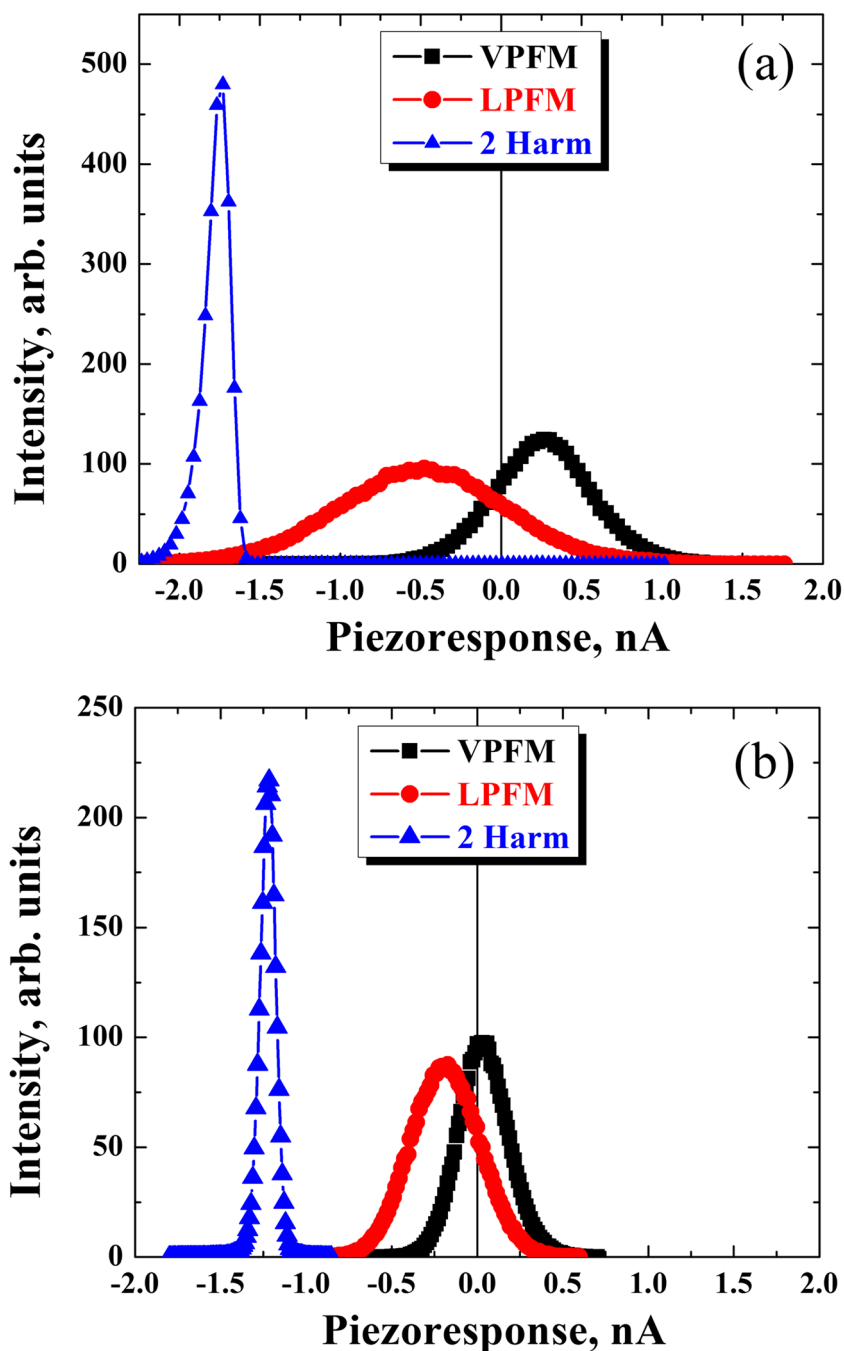


Fig. 7 Distributions of the local piezoelectric response (vertical (VPFM) and lateral (LPFM) signals) and second harmonic signal (2 Harm) in samples I (a) and V (b) obtained from Fig. 6



of the signal of the second harmonic must decrease, too, that is observed in the experiment (Fig. 7).

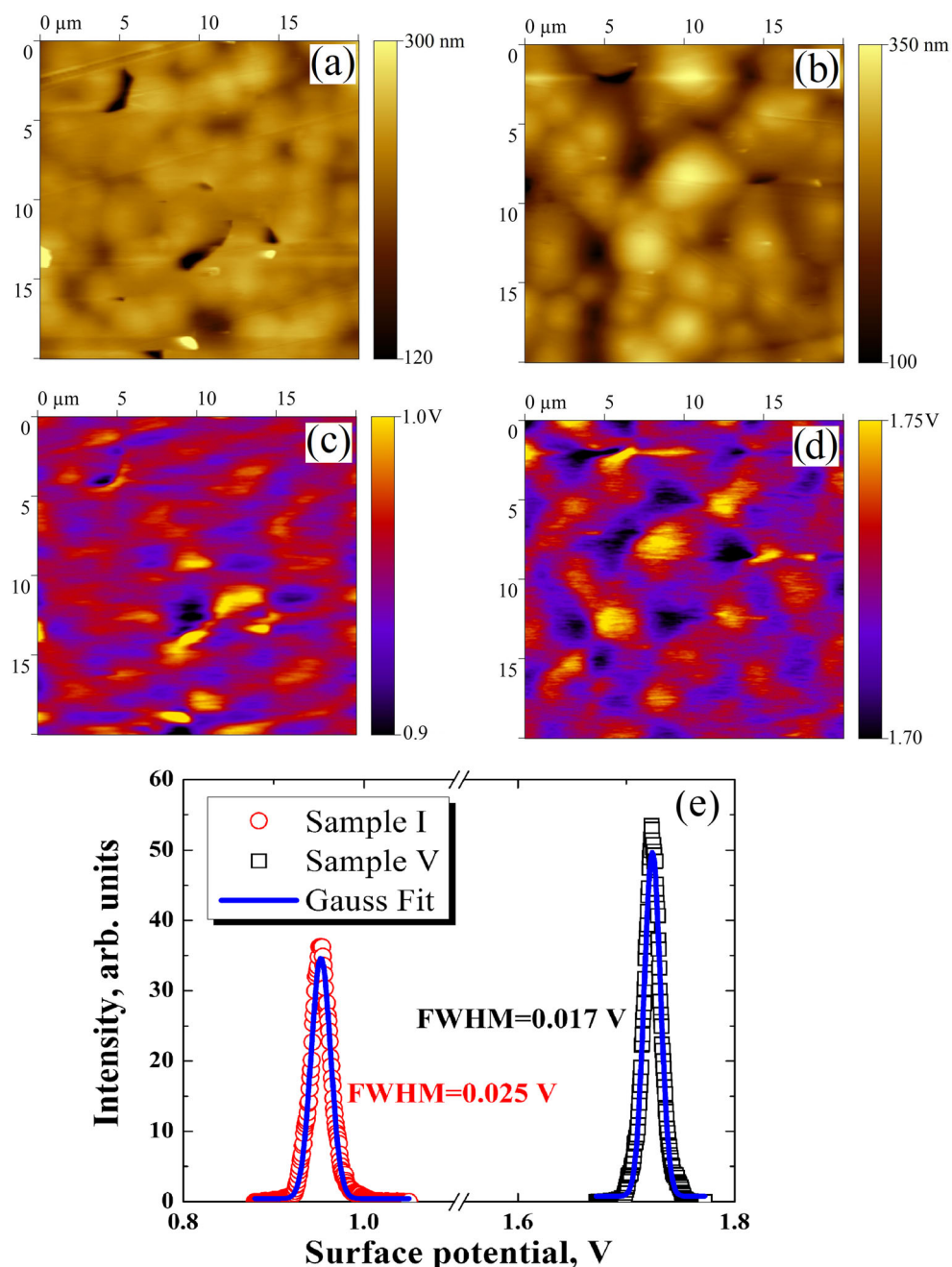
Another conclusion also follows from this picture. For sample V, distribution curves get narrower. Thus, chain enrichment of PVDF chains with isomers in the conformation of a planar zigzag noted earlier results in more uniform distribution of domains. Width values of full-width-at-half-maximum (FWHM) distribution curves listed in the table at histograms presented in Table 4 allow it to be seen quantitatively.

In Fig. 8, scans topography (a and b), surface potential (c and d), and their distribution histograms for the original (I) and

Table 4 The FWHM values obtained from histograms presented in Fig. 7

No.	Parameter FWHM		
	VPFM (nA)	LPFM (nA)	2 Harm (nA)
Sample I	0.70 ± 0.01	1.21 ± 0.01	0.18 ± 0.01
Sample V	0.39 ± 0.01	0.48 ± 0.01	0.11 ± 0.01

Fig. 8 Topography (a, b), signals of the surface potential (c, d), and histograms of the surface potential distribution (e) for samples I и V, respectively



doped film (V) are shown. Histograms presented here show that the doped film areas of positive charge localization have the narrower distribution (Fig. 8e). As it follows from aforesaid, the same effect also took place for domain size distribution (Fig. 7). For the same films, loops of piezoelectrical hysteresis obtained in SS-PFM regime are presented in Fig. 9. For non-doped films, strong curve asymmetry at SS-PFM to y-axis is presented. As it follows from our earlier data, the curve shift noted above must be connected with the formation of the space charge field [44]. The presence of crystals, containing two phases in the non-doped film, may be the cause of

stronger asymmetry of piezo-electrical hysteresis. It may be the result of the presence of various polar planes, which are deep traps for quasi-free carriers in a polymer. Apparently, film doping lowering the proportion of the γ phase decreases this asymmetry (Fig. 9, curve for sample V). Simultaneously, it may be seen that an increase in a number of chains in the conformation of a planar zigzag in such sample is accompanied by lowering of the coercive field.

The radial field distribution is given by the following expression, which is obtained under the assumption that the tip is a charged sphere [45]:

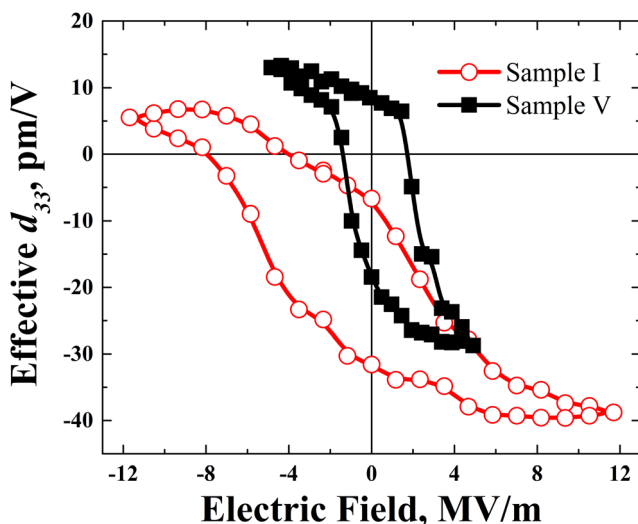


Fig. 9 Remnant PFM hysteresis for samples I and V

$$E(r) = \frac{C_t U_t}{2\pi\epsilon_0(\sqrt{\epsilon_c\epsilon_a} + 1)} \cdot \sqrt{\frac{\epsilon_a}{\epsilon_c}} \cdot \frac{R + \delta}{[(R + \delta)^2 + r^2]^{3/2}} \quad (2)$$

Here, r is the distance from the tip along the surface (228 nm for sample I and 273 nm for sample V at maximum DC voltage), R is the probe tip radius (30 nm), δ is the tip distance from the surface, C_t is the capacitance of the system consisting of the tip and the dielectric semi-infinite crystal, and ϵ_c and ϵ_a are relative permittivity values of the polymer sample along polar and non-polar directions, respectively.

As it follows from Fig. 9, values of coercive fields turn to be about two orders of magnitude lower than those in work [10], where the PVDV film with IL had extremely high coercive field (~ 200 MB/m). Such a difference may have various causes. One of them is associated with the fact that hysteresis loops obtained by us and in work [10] have been received by different methods. Another cause may be connected with the difference in the thickness of films: in our case, it was 30 μm while in work [10] thickness was 0.43 μm . We used Ag electrodes while in the cited work Al electrodes were used. As it was shown by us recently, in the last case, the formation of new functional groups is possible. They shift experimentally observed coercive field to greater values [46]. At a low thickness of the film measured, surface effects will be higher. That is why in work [10] such high coercive fields could be observed.

Conclusion

It has been found that introduction of organic ionic liquids in the solution of ferroelectric polyvinylidene fluoride (PVDF) results in the growth of a number of its isomers in the form of a planar zigzag at crystallizing of this polymer.

Simultaneously an increase in the crystallinity degree is observed. By the method of local piezoresponse force microscopy, it was found that this process is accompanied by a change in its domain structure. It comes to the fact that the domain size distribution gets narrower. The distribution of domains of the surface potential changes, too. It was found that the mechanism of piezoelectricity in PVDF should have a high contribution to the effect of electrostriction, which is determined by the response to the external influence of the chains of the amorphous phase. This is proved by the fact that as the crystallinity of the films increases, the piezoelectric response signal on the second harmonic decreases. Curves of piezoelectrical hysteresis have strong asymmetry which decreases at polymer crystallizing in the presence of ionic liquid. It was shown that doped films of ferroelectric PVDF have the lower coercive field than non-doped ones.

Acknowledgments The work is supported by RFBR project 18-03-00493. PFM and KPFM studies were performed at Center for Shared Use “Material Science and Metallurgy” at the National University of Science and Technology “MISIS” and were supported by the Ministry of Science and Higher Education of the Russian Federation (state tasks 11.9706.2017/7.8 and 16.2811.2017/4.6).

Compliance with ethical standards

Conflict of interest The authors declare that they have no conflict of interest.

References

1. Wang TT, Herbert JM, Glass AM (eds) (1988) The application of ferroelectric polymers. Blackie, Glasgow
2. Nalva HS (ed) (1995) Ferroelectric polymers – chemistry, physics and applications. Marcel Dekker Inc, New York
3. Kochervinskii VV (1994) The properties and applications of fluorine-containing polymer films with piezo- and pyro-activity. Russ Chem Rev 63(4):367
4. Kochervinskii VV (1996) Structure and properties of bulk polyvinylidene fluoride and systems based on it. Russ Chem Rev 65(10):865–913
5. Kochervinskii VV (1999) Ferroelectricity of polymers based on vinylidene fluoride. Russ Chem Rev 68(10):821–857
6. Kochervinskii VV, Shoranova LO, Bondarenko SA, Afonkin AE (2016) Applications of ferroelectric polymers as membranes, proton conductive materials and in gel polymer electrolytes. Int J Pharm Technol 8(4):27238–27265
7. Tokuda H, Tsuzuki S, Susan ABH, Hayamizu K, Watanabe M (2006) How ionic are room-temperature ionic liquids? An indicator of the physicochemical properties. J Phys Chem B 110:19593–19600
8. Moriyasu T, Sakamoto T, Sugihara N, Sasa Y, Ota Y, Shimomura T, Sakai Y, Ito K (2013) Ionic conduction of slide-ring gel swollen with ionic liquids. Polymer. 54:1490–1496
9. Wang J, Fu Q, Zhang Q (2012) Inducing of dominant polar forms in poly(vinylidene fluoride) with super toughness by adding alkyl ammonium salt. Polymer. 53:5455–5458

10. Wang F, Lack A, Xie Z, Frubing P, Taubert A, Gerhard R (2012) Ionic-liquid-induced ferroelectric polarization in poly(vinylidene fluoride) thin films. *Appl Phys Lett* 100:062903 (1–4)
11. Tazaki M, Wada R, Okabe M, Homma T (2000) Inverse gas chromatographic observation of thermodynamic interaction between poly(vinylidene fluoride) and organic solvents. *Polym Bull* 44: 93–100
12. Gregorio R, Cestari M (1994) Effect of crystallization temperature on the crystalline phase content and morphology of poly(vinylidene fluoride). *J Polym Sci B Polym Phys* 32:859–870
13. Gregorio R, Botta MM (1998) Effect of crystallization temperature on the phase transitions of P(VDF/TrFE) copolymers. *J Polym Sci B Polym Phys* 36:403–414
14. Gregorio R (2006) Determination of the α , β , and γ crystalline phases of poly(vinylidene fluoride) films prepared at different conditions. *J Appl Polym Sci* 100:3272–3279
15. Gregorio R, Borges DS (2008) Effect of crystallization rate on the formation of the polymorphs of solution cast poly(vinylidene fluoride). *Polymer*. 49:4009–4016
16. Hasegawa R, Takahashi Y, Chatani Y, Tadokoro H (1972) Crystal structures of the three crystalline forms of polyvinylidene fluoride. *Polym J* 3:600–610
17. Kobayashi M, Tashiro K, Tadokoro M (1975). *Macromolecules* 8: 158
18. Bachmann MA, Koenig JL (1981) Vibrational analysis of phase III of poly(vinylidene fluoride). *J Chem Phys* 74(10):5896–5910
19. Tashiro K, Takano K, Kobayashi M, Chatani Y, Tadokoro H (1984) Structural study of ferroelectric phase transition of vinylidene fluoride-trifluoroethylene copolymers. III. Dependence of transitional behavior on VDF molar content. *Ferroelectrics* 57: 297–326
20. Kochervinskii VV (2006) Structural changes in ferroelectric polymers under the action of strong electric fields by the example of polyvinylidene fluoride. *Crystallogr Reports (Russia)* 51:S88–S107
21. Priya L, Jog JP (2002) Poly(vinylidene fluoride)/clay nanocomposites prepared by melt intercalation: crystallization and dynamic mechanical behavior studies. *J Polym Sci B Polym Phys* 40:1682–1689
22. Priya L, Jog JP (2003) Intercalated poly(vinylidene fluoride)/clay nanocomposites: structure and properties. *J Polym Sci B Polym Phys* 41:31–38
23. Priya L, Jog JP (2003) Polymorphism in intercalated poly(vinylidene fluoride)/clay nanocomposites. *J Appl Polym Sci* 89:2036–2040
24. Ramasundaram S, Yoon S, Kim KJ, Park C (2008) Preferential formation of electroactive crystalline phases in poly(vinylidene fluoride)/organically modified silicate nanocomposites. *J Polym Sci B Polym Phys* 46:2173–2187
25. Buckley J, Cebe P, Cherdack D, Crawford J, Ince BS, Jenkins M, Pan J, Reveley M, Washington N, Wolchover N (2006) Nanocomposites of poly(vinylidene fluoride) with organically modified silicate. *Polymer*. 47:2411–2422
26. Dillon DR, Tenneti KK, Li CY, Ko FK, Sics I, Hsiao BS (2006) On the structure and morphology of polyvinylidene fluoride–nanoclay nanocomposites. *Polymer*. 47:1678–1688
27. Ince-Gunduz BS, Alpern R, Amare D, Crawford J, Dolan B, Jones S, Kobylarz R, Reveley M, Cebe P (2010) Impact of nanosilicates on poly(vinylidene fluoride) crystal polymorphism: part 1. Melt-crystallization at high supercooling. *Polymer* 51:1485–1493
28. Martins P, Costa CM, Lanceros-Mendez S (2011) Nucleation of electroactive β -phase poly(vinylidene fluoride) with CoFe_2O_4 and NiFe_2O_4 nanofillers: a new method for the preparation of multiferroic nanocomposites. *Appl Phys A Mater Sci Process* 103:233–237
29. Martins P, Costa CM, Benelmekki M, Botelho G, Lanceros-Mendez S (2012) On the origin of the electroactive poly(vinylidene fluoride) β -phase nucleation by ferrite nanoparticles via surface electrostatic interactions. *Cryst Eng Comm* 14:2807–2811
30. Sencadas V, Martins P, Pitaes A, Benelmekki M, Gomez Ribelles JL, Lanceros-Mendez S (2011) Influence of ferrite nanoparticle type and content on the crystallization kinetics and electroactive phase nucleation of poly(vinylidene fluoride). *Langmuir* 27:7241–7249
31. Yi Z, Zhu L-P, Zhang H, Zhu B-K, Xu Y-Y (2014) Ionic liquids as co-solvents for zwitterionic copolymers and the preparation of poly(vinylidene fluoride) blend membranes with dominated β -phase crystals. *Polymer*. 55:2688–2696
32. Li Y, Xu J-Z, Zhu L, Xu H, Pan M-W, Zhong G-J, Li Z-M (2014) Multiple stage crystallization of gamma phase poly(vinylidene fluoride) induced by ion-dipole interaction as revealed by time resolved FTIR and two-dimensional correlation analysis. *Polymer*. 5:4765–4775
33. Bazhenov AV, Fursova TN, Turanov AN, Aronin AS, Karandashev VK (2014) Properties of a composite material based on multi-walled carbon nanotubes and an ionic liquid. *Phys Solid State* 56(3):572–579
34. Lassegues J-C, Grondin J, Cavagnat D, Johansson P (2009) New interpretation of the CH stretching vibrations in imidazolium-based ionic liquids. *J Phys Chem A* 113(23):6419–6421
35. Kochervinskii VV, Kozlova NV, Shmakova NA, Kalabukhova AV, Kiselev DA, Malinkovich MD, Gradova MA, Gradov OV, Bedin SA (2018) Influence of dye molecules on the polarization of ferroelectric vinylidene fluoride copolymer. *Crystallogr Rep* 63(6):983–988
36. Kochervinskii VV, Gradova MA, Gradov OV, Kiselev DA, Iliina TS, Kalabukhova AV, Kozlova NV, Shmakova NA, Bedin SA (2019) Structural, optical, and electrical properties of ferroelectric copolymer of vinylidene fluoride doped with Rhodamine 6G dye. *J Appl Phys* 125:044103 (1–9)
37. Kalinin SV, Shao R, Bonnell DA (2005) Local phenomena in oxides by advanced scanning probe microscopy. *J Am Ceram Soc* 88(5):1077–1098
38. Shao R, Bonnell DA (2004) Scanning probes of nonlinear properties in complex materials. *Jpn J Appl Phys* 43(7B):4471–4476
39. Kochervinskii VV (2003) Piezoelectricity in crystallizing ferroelectric polymers: polyvinylidene fluoride and its copolymers (a review). *Crystallogr Rep* 48(4):649–675
40. Kochervinskii VV (2009) New electrostriction materials based on organic polymers: a review. *Crystallogr Rep Suppl* 54(7):1146–1171
41. Furukawa T, Seo N (1990) Electrostriction as the origin of piezoelectricity in ferroelectric polymers. *Jpn J Appl Phys* 29:675–680
42. Tasaka S, Miyata S (1981). *Ferroelectrics* 32:17
43. DveyAharon H, Sluckin TJ, Taylor PL (1981). *Ferroelectrics* 32:25
44. Kochervinskii VV, Chubunova EV, Lebedinskii YY, Pavlov AS, Pakuro NI (2015) Influence of the high-voltage conductivity on peculiarity of polarization ferroelectric polymer on based vinylidene fluoride. *Adv Mater Res* 4(2):113–132
45. Molotskii M, Agronin A, Urenski P, Shvelbelman M, Rosenman G, Rosenwaks Y (2003) Ferroelectric domain breakdown. *Phys Rev Lett* 90(10):107601
46. Kochervinskii VV, Chubunova EV, Bedin SA (2018) An effect of electrode material on pinning layer characteristics and depolarization field in polymer ferroelectrics. *J Appl Phys* 124(6):064102 (1–6)

Publisher's note Springer Nature remains neutral with regard to jurisdictional claims in published maps and institutional affiliations.